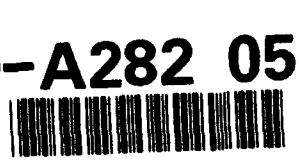

ARMY RESEARCH LABORATORY

Review of Light Scattering Literature

Marie K. Potts

ARL-TR-453

June 1994

The findings in this report are not to be construed as an official Department of the Army position unless so designated by other authorized documents.

Citation of manufacturer's or trade names does not constitute an official endorsement or approval of the use thereof.

Destroy this report when it is no longer needed. Do not return it to the originator.

REPORT DOCUMENTATION PAGE

Form Approved
OMB No. 0704-0188

1. AGENCY USE ONLY (Leave blank)	2. REPORT DATE	3. REPORT TYPE AND DATES COVERED
	June 1994	Final Report

4. TITLE AND SUBTITLE
Review of Light Scattering Literature

5. FUNDING NUMBERS

6. AUTHOR(S)
Marie K. Potts

7. PERFORMING ORGANIZATION NAME(S) AND ADDRESS(ES)
U.S. Army Research Laboratory
Watertown, MA 02172-0001
ATTN: AMSRL-MA-PB

8. PERFORMING ORGANIZATION REPORT NUMBER
ARL-TR-453

9. SPONSORING/MONITORING AGENCY NAME(S) AND ADDRESS(ES)
U.S. Army Research Laboratory
2800 Powder Mill Road
Adelphi, MD 20783-1197

10. SPONSORING/MONITORING AGENCY REPORT NUMBER

11. SUPPLEMENTARY NOTES

12a. DISTRIBUTION/AVAILABILITY STATEMENT
Approved for public release; distribution unlimited.

12b. DISTRIBUTION CODE

13. ABSTRACT *(Maximum 200 words)*

This report reviews the recent literature of static and dynamic light scattering of dilute and semidilute polymer solutions and gels, as obtained from the Chemcial Abstracts Macromolecular Sections, and an electronic literature search. In general, this review has been confined to the interests of the Polymer Research Branch, specifically experimental light scattering studies of synthetic polymers in solution. In order to further limit the size of this review, light scattering for phase separation studies or particle size analysis have been excluded, as well as light scattering used strictly for size exclusion chromatography detection.

14. SUBJECT TERMS	15. NUMBER OF PAGES
Light scattering, Polymer solutions	27
	16. PRICE CODE

17. SECURITY CLASSIFICATION OF REPORT	18. SECURITY CLASSIFICATION OF THIS PAGE	19. SECURITY CLASSIFICATION OF ABSTRACT	20. LIMITATION OF ABSTRACT
Unclassified	Unclassified	Unclassified	UL

NSN 7540-01-280-5500

Standard Form 298 (Rev. 2-89)
Prescribed by ANSI Std. Z39-18
298-102

Contents

1. Introduction

1.1. Purpose

The Polymer Research Branch (PRB) conducts fundamental research in the areas of polymer synthesis and characterization for materials of potential use to the U.S. Army. Part of this effort is to remain cognizant of developments in our areas of expertise and related fields. PRB currently has the capability to analyze polymer solutions via static and dynamic light scattering for structural information. This review focuses on published papers of that genre.

1.2. Light Scattering Theory

Classical electromagnetic theory tells us that incident light which impinges on a nonconducting, nonmagnetic, nonabsorbing molecule induces a fluctuating dipole in the molecule which then radiates light of the same frequency in all directions. In the case of polymer solutions, this elastically scattered light contains information on the size and shape of the scattering molecules (static light scattering). However, the light is not only scattered elastically, but also inelastically (Brillouin and Raman scattering) and quasielastically (dynamic light scattering) by the motions of the polymers in solution due to the Doppler effect. In the case of Brillouin and Raman scattering, the frequency of the scattered radiation is shifted from the incident frequency by sound waves in the fluid (Brillouin) and vibrational motions of the molecules (Raman). Dynamic light scattering, also called quasielastic light scattering (QELS) or photon correlation spectroscopy (PCS), is the study of the very small shifts of the Rayleigh (elastic) scattered light caused by the translations and rotations of molecules. These shifts are on the order of 10^{-5} cm^{-1} (compared to 1000 cm^{-1} for Raman spectroscopy), too small to be measured by standard spectroscopic techniques, and thus are usually measured in the Fourier-transformed time domain using correlation functions (hence the term photon correlation spectroscopy).

Dynamic light scattering (DLS) determines the frequency distribution of the scattered light at a given angle, $I(\omega,\theta)$, whereas static light scattering (SLS) involves measurement only of the total intensity of light scattered at that angle, $I(\theta)$, essentially the integration of the DLS spectrum over the entire frequency range.

1.2.1. Dynamic Light Scattering

The scattered light impinging on a photomultiplier tube (PMT) outputs a current, i(t), which is proportional to the intensity of the scattered light, $I_S(t)$. Since the intensity of the light is equal to the square of the electric field, $I_S(t) = E_S(t)^2 \propto i(t)$. The output of the PMT is then fed into a correlator which computes the intensity autocorrelation function,

$$\langle i(0)i(\tau)\rangle = B \langle |E_S(0)|^2 |E_S(\tau)|^2 \rangle, \qquad (1)$$

where B is a proportionality constant. This correlation function is similar to an exponential decay curve, and a single (or distribution of) characteristic decay times (τ_C) can be extracted via data analysis routines. The Fourier transform of this correlation function is the power spectrum or spectral density, and τ_C is related to the linewidth of the power spectrum through $\Gamma = 2\pi/\tau_C$. This linewidth (or distribution of linewidths) can be related to the rotational and translational diffusion causing the line broadening of the Rayleigh scattered light. For simple translational diffusion, each Γ is related to a translational diffusion coefficient D_T, which is related to the hydrodynamic size of the scattering molecule. Thus, DLS can be used to determine particle size distributions or in certain cases, molecular weight distributions.

The scattered electric field is proportional to the molecular polarizability of the molecule, $\alpha(t)e^{iq\cdot r(t)}$. This tensor has two components: $\alpha(t)$, the polarizability of the molecule along the initial and final polarization directions, and $e^{iq\cdot r(t)}$, the component which changes as the molecule translates, where r(t) is the molecule's position at time t. The scattering wave vector (q) is defined as $(4\pi n/\lambda)\sin(\theta/2)$, where λ is the wavelength of the scattering radiation, n is the refractive index of the scattering medium, and θ is the angle at which the scattered light is detected.

When the product of the wave vector and the radius of the scattering particle is less than unity ($qR << 1$, usually the case for synthetic macromolecules using visible radiation), the time correlation function is sensitive to fluctuations occurring on the time-scale associated with center-of-mass diffusion. In this case, the diffusion coefficient of the molecule can be simply related to the experimentally determined linewidth via $\Gamma = Dq^2$. If spherical particles are assumed, the Stokes-Einstein equation can be used to convert D to a hydrodynamic radius, R_h.

When qR exceeds unity (particles are very large, or scattering is from shorter wavelength radiation or is detected at large angles), the motions of the scattering particle cannot be attributed to translational diffusion alone, internal motions of the particle become important, and rotational diffusion coefficients (Θ) may be calculated.

In many applications of dynamic light scattering, the interpretation of the experimentally determined linewidths cannot be simply related to translational and rotational diffusion coefficients or to particle sizes. However, it is still useful to determine the distribution of linewidths, particularly when there are bimodal distributions present, because it is an indication of different size particles, which might be interpreted as due to aggregation or other phenomenon.

1.2.2. Static Light Scattering

Classical electromagnetic theory and solution thermodynamics show that the intensity of light scattered from a polarized light source of wavelength λ by small, isotropic scatterers at an angle θ can be represented by

$$\frac{Kc}{R_\theta} = \frac{1}{M_w} + 2A_2c + 3A_3c^2 + \cdots \qquad (2)$$

In the above equation, the Rayleigh ratio, R_θ, is proportional to the intensity of the scattered light at angle θ, c represents the solution concentration, and K is an optical constant which contains the refractive index of the solvent, the differential refractive index (dn/dc) of the solution over the solvent, and the wavelength of scattering radiation, λ. The second and third virial coefficients, A_2 and A_3, are related to the thermodynamic quality of the solution. When A_2 is positive, the solvent is thermodynamically more favorable to the polymer segments than other polymer segments, thus the polymer in solution adopts a configuration more extended than in the bulk, whereas a negative A_2 value implies a contracted configuration. When A_2 is zero, the polymer configuration is the same as in the bulk, since the solvent is neither favored nor unfavored - this condition is called the theta (Θ) state, and the solvent is termed a Θ solvent.

For larger particles ($R > 1/20\ \lambda$), the light scatters off different parts of the same molecule, and an angular dependence of the scattered light is observed, from which the root mean square radius of gyration (R_g, or $\langle s^2 \rangle_z^{1/2}$) may be determined:

$$\frac{Kc}{R\theta} = \frac{1}{M_w}\left(1 + \frac{16\pi^2}{3\lambda^2} R_g^2 \sin^2\left(\frac{\theta}{2}\right) + \cdots\right). \qquad (3)$$

where the ellipsis indicates higher order terms in $R_g^2 \sin^2(\theta/2)$ may be included.

Typically, static light scattering measurements of several solution concentrations are carried out, and if the scattering due to solvent alone (measured in a separate experiment) is subtracted, one obtains a series of $R_{\theta,c}$ values which can be analyzed via a Zimm Plot. In this case, $Kc/R_{\theta,c}$ is plotted on the ordinate vs. $\sin^2(\theta/2) + kc$ on the abscissa, where k is an arbitrary constant. This plot produces a series of points which resemble a grid. Lines can be fit to points of constant concentration and extrapolated to zero angle. The points representing a constant angle (θ) can also be extrapolated to zero concentration. The two sets of extrapolated points can then each be extrapolated to a common point, representing zero angle and concentration, which is the zero-intercept of the plot. This intercept is the reciprocal of the weight average molecular weight, M_W. The second virial coefficient A_2 and sometimes the third virial coefficient, A_3 can be determined from the slope of the zero-angle line, and the z-average root mean square radius of gyration, R_g or $\langle s^2 \rangle_z^{1/2}$ may be determined from the slope of the zero-concentration line.

The weight-average molecular weight M_W determined from SLS experiments is an absolute quantity, independent of the solvent used. The virial coefficients and the radii of gyration, however are thermodynamic parameters, and thus are solvent and temperature dependent.

Intrinsic viscosities [η] are often reported in conjunction with light scattering results. [η] is the viscosity of a polymer solution which has been corrected for solution concentration and solvent viscosity, and thus can be a measure of size in solution, depending on the draining characteristics of the polymer. The logarithm of the viscosity average molecular weight, M_V, is proportional to the log of [η] for a homologous series of polymers in a particular solvent. This proportionality can be expressed mathematically by a Mark-Houwink-Sakurada equation of the form

$$[\eta] = k M_V^a \qquad (4)$$

where the pre-exponential factor and the exponent are unique to that polymer/solvent combination. The weight average molecular weight is close in value to M_V, thus light scattering is often used to compute the molecular weights for this equation.

2. Static Light Scattering Papers (SLS)

This section reviews papers that deal only with static light scattering of polymers.

2.1. Dilute Solution Properties of Homopolymers

A Mark-Houwink-Sakurada (M-H-S) equation for polyurethane in benzene has been proposed by Ali [1] for a polyurethane prepared by reacting equimolar proportions of butanediol and hexamethylene diisocyanate. The polymer was separated into eight fractions with a molecular weight range of 4,000 to 60,000 by fractional precipitation with 2,2,4-trimethylpentane. Each fraction was analyzed via low angle laser light scattering and intrinsic viscosity in benzene solution, and the refractive index increment was determined to be 0.034 ml/g. A log-log plot of

[η] vs. M_w was linear, yielding a pre-exponential value of 2.45 x 10^{-4} dL/g and an exponent of 0.70 for the M-H-S equation.

Dilute solution properties of ultrahigh molecular weight polymers (M_w ~ 20 - 30 million) are reported by Bercea, et al. [2] for the polymers polymethylmethacrylate (PMMA), polybutylmethacrylate (PBMA) and polyacrylonitrile (PAN). They observed some unusual properties for these high molecular weight materials such as (1) low molecular weight and compositional heterogeneity for copolymers; (2) less conformational changes as a function of temperature and solvent changes; and (3) an increased rigidity in solution as evidenced by the dependence of the radius of gyration, second virial coefficient and intrinsic viscosity on the molecular weight. This paper is essentially a compilation of 11 previous papers which were detailed structural studies. Calculating the branching index by comparing measured values of the radius of gyration and intrinsic viscosity with calculated values for linear polymers, the authors conclude that the unusual properties are not due to branching for PMMA and PBMA, but the evidence for PAN is unclear. They don't speculate on precisely what the causes of the unusual properties are, but they feel that they are unique to the long chain nature of these polymers.

In a short note, Gooda and Huglin [3] report dilute solution properties (via light scattering, membrane osmometry and intrinsic viscosity measurements) on a new water-soluble neutral polymer, poly(2-acrylamido-2-methylpropanesulfonamide), PAMAS. This polymer was prepared from the corresponding sulfonic acid (PAMS) by amidation with formamide. The PAMAS polymer was fractionated into 14 components, of which 9 were characterized in water and formamide, both of which are thermodynamically good solvents. The major conclusions drawn from the work are that the polymer is a flexible coil in good solution, yet calculation of steric factors and characteristic ratios would indicate a rather stiff chain. The absence of electrolyte behavior was also confirmed.

Nakamura and coworkers [4] have reported on the dependence of the second (A_2) and third (A_3) virial coefficients on molecular weight for poly(isobutylene) in cyclohexane solution. This is an extension of the work previously reported for polystyrene in benzene, in which A_3 scaled with the molecular weight to the power of 0.6, and the reduced third virial coefficient, $A_3/(A_2^2 M_w)$, was proportional to M_w. This study was an attempt to determine the universality of these relations for long flexible polymers in good solvents. Similar results were obtained for the PIB/cyclohexane system, but no available theories were found to predict this behavior.

Oun [5] published a paper on the solution properties of branched and unbranched polystyrene in good and theta solvents using static light scattering. The linear polystyrene (PS) samples used were standards obtained from three different sources. Two different branched PS samples were prepared by copolymerizing divinylbenzene with styrene: sample B which was a low conversion, lightly branched polymer, prepared by precipitating half of the reaction mixture after 1 1/2 hours polymerization, and sample A, a high conversion, highly branched polymer, which was allowed to react for an additional two hours. The resulting polymers were subsequently separated into 13 and 9 fractions, respectively, by precipitation with isopropanol, of which 3 from each series were selected for characterization by light scattering. The Flory expansion factor, $\alpha_s = \langle s^2 \rangle^{1/2} / \langle s^2_\theta \rangle^{1/2}$, were calculated for the branched fractions, based on radii of gyration obtained from light scattering in good (THF) and theta (cyclohexane) solvents, and compared with the viscosity expansion factor, α_η^3, the ratio of the intrinsic viscosity in a good and theta solvent. The expansion factors have been shown to be related to each other via $\alpha_\eta^3 = \alpha_s^{2.43}$, although in the present study, only 2 of the 6 samples studied (from the B series) followed this equality. The branching factor g_s was calculated by computing the ratio of the radius of gyration of a branched polymer to the radius of a linear polymer of the same molecular

weight. These factors agreed with theoretical estimates of g_S for the same two polymers for which the expansion factors agreed. The author suggests that since fractionation occurs for both molecular weight and branching, perhaps these samples are too nonuniform in terms of molecular weight distribution and structure to apply the theoretical expressions.

2.2. Polyelectrolytes

Griebel and Kulicke [6] described the characterization of water-soluble cationic polyelectrolyte copolymers via light scattering and intrinsic viscosity in 1M NaCl aqueous solutions. Three different copolymer systems were studied in which the compositions of the comonomers were varied, but in all cases, the first comonomer was poly(acrylamide). The other comonomers were chlorine salts of trimethyl ammonium ethyl-acrylate and -methacrylate, and trimethyl ammonium propyl-acrylamide. The authors determined the Mark-Houwink-Sakurada constants and the corresponding constants for the radius of gyration/molecular weight relationship. The exponent of the Mark-Houwink expression was found to increase as the composition of the cationic comonomer increased, probably due to increased electrostatic interaction and steric considerations. They compared their experimental numbers to calculated values using the Flory-Fox constant of 2.1×10^{21} for polyelectrolytes. The agreement between experimental and calculated values was not very good, even when corrections for polydispersity were incorporated. The authors concluded that the use of a universal constant for polyelectrolytes, irrespective of chemical structure and charge density is probably not valid.

Hunkeler, et al. [7] report on a light scattering method for molecular weight characterization of poly(acrylamide-co-sodium acrylate). A series of narrow molecular weight distribution polymers (MW varying from 10,000 to 1,000,000) were prepared from a large scale fractional precipitation of polyacrylamide. They were hydrolyzed to varying degrees to produce copolymers with 5 to 35% sodium acrylate content. A method was developed to characterize these copolymers in a high ionic strength aqueous solution using low angle laser light scattering (LALLS). The refractive index increment at constant chemical potential was determined (using dialysis) for several different sodium acrylate contents, from which a curve was constructed to determine the refractive index of any copolymer with a know chemical composition. The optimum dialysis time was determined by monitoring the refractive index of a copolymer solution during dialysis and determining the time required for the refractive index to stabilize. The molecular weights determined from this polyelectrolyte method were compared to molecular weights determined on the nonionic homopolymers and compared favorably (±10%, which is reasonable for aqueous light scattering) demonstrating the validity of the method.

Mattoussi and coworkers [8] have reported a light scattering study on the dilute solution properties of poly(xylylene tetrahydrothiophenium chloride), precursor to poly(*p*-phenylenevinylene), PPV, which is insoluble in common solvents. Experimentally determined radii of gyration and second virial coefficients were found to have a strong negative dependence on the counterion concentration, consistent with the postulation that the counterion screens the electrostatic repulsive interactions between ions on the polyelectrolyte. The R_g and A_2 values were found to be proportional to the reciprocal of the counterion concentration (C_S), although in the case of the second virial coefficient, this linearity was only present for very high ionic strengths. This behavior can be attributed to a flexible wormlike chain with electrostatic contributions to the persistence length. Theoretical expressions were formulated to describe the slope of plots of R_g and A_2 vs. $1/C_S$ in terms of the persistence length of the neutral polymer and the Bjerrum length (related to the Debye-Huckel screening parameter). The experimental values obtained from plots of R_g and A_2 vs. $1/C_S$ were only qualitatively in agreement with theoretical predictions. Light scattering and refractive index increment measurements in salt solution were not made at constant chemical potential, so this may have some effect on the experimental results.

Nordmeier and Dauwe [9] investigated the thermodynamic properties of dilute polyelectrolyte solutions via dialysis equilibrium and static light scattering studies. The combination of these two techniques provides information on the number of charges per polyion, Z_e, and the effects these charges have on the dilute solution properties of the polyion. The authors have ascertained that sodium polystyrenesulfonate in dilute solution behaves like a flexible worm-like coil whose dimensions increase upon lowering the ionic strength, which is caused by an increase in Z_e. Measurements of the second virial coefficient were in qualitative agreement with two currently available theories in which the polyelectrolyte is approximated as (1) a neutral sphere (which works only at low Z_e), or (2) a uniformly charged rigid cylinder. The authors plan to modify the latter theory to incorporate chain flexibility.

2.3. Copolymers and Polymer Mixtures

Light scattering measurements are reported by Ould-Kaddour and Strazielle 10] for incompatible mixtures of polystyrene-PMMA in a good solvent (toluene or benzene) and for polystyrene-poly(vinyl acetate) in the good solvent styrene. They examined the angular distribution of scattered intensity (which is rather unusual for a polymer mixture) as well as the thermodynamic properties of the two unlike polymers. The molecular weights and concentrations of the two polymers were varied over a large range. The angular distribution data obtained for a polymer mixture reveals apparent dimensions, which depended on the proportion of the two polymers.

Quintana, et al. reported a two-part study on the micellization of a polystyrene-block-poly(ethylene/propylene) copolymer in n-alkane solutions using light scattering and viscometry. The first paper [11] is a thermodynamic study in which light scattering is used to determine the dependence of the micelle/free chain equilibrium on temperature and concentration. Measurements of critical micelle temperature for various concentrations of copolymer yielded values of the standard free energy, entropy and enthalpy of micellization in the various n-alkanes (6 - 12 carbons). In contrast to micromolecular surfactants in aqueous media, enthalpy is the force driving the micellization process for block copolymers in aqueous media, since the entropy of the process (chains becoming more compact) is negative. The enthalpy of micellization was shown to become more negative with increasing carbon-number of the alkane, due to the fact that the increase in the alkane chain reduces the solubility for the polystyrene block of the copolymer, thereby favoring micelle formation. On the other hand, the entropy of micellization was found to become more negative (less favorable) with increasing carbon number. This effect was explained by the fact that the cores of block copolymer micelles contain solvent molecules, which increases the entropy of the system, and the polystyrene core can adsorb *n*-hexane and *n*-heptane molecules under certain conditions, but not the higher alkanes.

The second part of Quintana's paper [12] is a structural study using light scattering and viscometry to determine weight-average molecular weights, radii of gyration, second virial coefficients, and hydrodynamic radii of the micelles as a function of the temperature and the carbon number of the alkane. Molecular weights were found to be independent of temperature, when the light scattering measurements were carried out above the critical micelle temperature. The effect of the solvent on the molecular weight depended on the temperature. At low temperature the molecular weights increased with increasing carbon-number, indicating an increase in micelle formation with a decrease in solvent quality, whereas at higher temperatures, a minimum in the molecular weight vs. carbon-number was observed for octane, which had the smallest ΔG value for micelle formation. Radii of gyration determined were smaller than expected for the corresponding molecular weights, indicating the compactness of the micelles. Viscosity measurements as a function of temperature showed little change as the critical micelle temperature was exceeded, but the measured viscosity was very dependent on the number of carbon atoms, showing a maximum value with heptane and a very low value in hexadecane.

3. Dynamic Light Scattering (DLS) and Combined SLS and DLS Papers

This section reviews papers which are primarily dynamic light scattering studies, but most DLS papers contain supporting static light scattering results.

3.1. Molecular Weight Distribution (MWD) Analysis

A novel approach for determining the absolute molecular weight distribution (MWD) of polymers is described by White and Vancso [13], using a combination of gel permeation chromatography (GPC), low-angle laser light scattering (LALLS) and dynamic light scattering. Typically, to transform a distribution of diffusion coefficients (D_o, as determined from DLS) to a MWD, the pre-exponential factor (k_T) and exponent (b) of the dynamic scaling law relating D_o and M must be known, in addition to the second virial coefficient for diffusion, k_D. This is usually done by a tedious process of determining D_o for a homologous series of monodisperse polymers, either by fractionating a polydisperse sample or obtaining monodisperse standards. This new procedure involves using GPC-LALLS to obtain an estimate of the diffusion average MW, M_D, on a polydisperse sample using an estimated value of b, and then using dynamic Zimm Plots (DZP) to determine the corresponding D_o and k_D values. The DZP's in turn provide a better value of k_T and b, in which the b value can be used to obtain a better estimate of M_D, and this continues in an iterative manner. The authors also introduce the concept of a polydispersity index M_D/M_W, which can be determined from light scattering (static and dynamic) alone. The authors demonstrated this technique by determining the MWD of polystyrene in THF and cyclohexane (good and theta solvents), and GPC/LALLS was used to confirm that $M_W < M_D < M_Z$.

3.2. Chain and Sphere Diffusion

Data previously reported on polyisobutylene chains and silica spheres diffusing through polyisobutylene-$CHCl_3$ solutions is reanalyzed by Phillies et al. [14] in consideration of the reptation model of polymer dynamics. The diffusion coefficient for probe particles, D_p, and polymer chains, D_{ch} exhibited the expected stretched exponential dependence on the matrix solution concentration, c, with a scaling exponent ν approximately equal to 0.75, in the range previously reported of 0.5 - 1.0. The scaling prefactor (α) of the stretched exponential for spheres scaled as the molecular weight of the matrix (M) to the 1/2 power. For the polymer chains, the effect of varying the molecular weight of the probe (P) was also examined. For $P \ll M$, α depends substantially on P and less on M, while for $P \gg M$, α has a very weak dependence on either P or M. The main point of this paper, however, was to examine spheres and chains of equivalent size diffusing in the same matrix to observe whether or not reptation by polymer probe chains was present. This is the first study comparing random coil polymers and globular particles diffusing through the same matrix. Polymer chains can move by reptation or Stokes-Einstein type diffusion while spheres can only diffuse. Reptation and diffusion are independent processes, therefore their effects on D should be additive. In an entangled system ($c > c^*$, P and M large), diffusion of P is expected to be slow, so that reptation should dominate, and theory predicts that for equivalent sized spheres and polymer chains, $D_{ch} \gg D_p$, and the ratio should increase with increasing matrix concentration. Phillies, et al. demonstrated that for similar sized large spheres and polymers diffusing through a small M matrix, $D_p > D_{ch}$, but the ratio remained constant throughout the concentration range studied. However, for smaller spheres and polymers diffusing through a large M matrix, the observed D_p was greater than D_{ch}, and the ratio increased dramatically as the matrix concentration increased, in complete contrast to the reptation prediction. The authors feel that under these conditions highly favorable for reptation, that reptation is not a significant process for polymers diffusing in semidilute solution.

Rotstein and Lodge [15] have reported an extensive study on diffusion of tracer polystyrene through toluene solutions and gels of poly(vinyl methyl ether). The gels were carefully synthesized in an attempt to achieve consistent mesh size. The diffusion was studied at different solution concentrations, and different tracer molecular weights. Some of the data obtained support the reptation model for diffusion, however the diffusivity scaled with the molecular weight with exponents of -2.7 to -2.8, not -2 as the reptation model predicts. Other theories were mentioned as possible explanations for some of the data, but no single theory fit all the observed results.

3.3. Homopolymer Solutions

3.3.1. Flexible Polymers

The translational diffusion of atactic 1,2-polybutadiene in THF was studied by Li, et al.. [16], to assess the effects of chain flexibility and unperturbed dimensions on the dynamics and draining behavior. In a note, they describe dynamic light scattering of a series of polybutadienes with 1,2 content varying from 25 to 73%. They found little difference in the dynamic properties of the different polybutadienes in that the log MW vs. log D points all fell on the same line, regardless of the 1,2 content (the range of molecular weights studied was less than a decade, however). They speculate that maybe the hydrodynamic volumes for the same molecular weight are equal (hydrodynamic volume is related to translational diffusion), even when the 1,2 contents are different. This may be possible by having a change in radius of gyration offset by a change in draining character when the 1,2 content is varied for the same molecular weight polymer.

Martin, et al. [17] studied the internal structure and dynamics of dilute linear polymers by probing the dynamic light scattering in the intermediate scattering region where $qR_g >> 1$. The intermediate scattering regime was reached by using high molecular weight polystyrene with a large radius of gyration. This study was an attempt to verify the predicted fractal (scaling) dimensions of polymer solutions, by extracting the exponents directly from the data without appealing to theories which fix the exponents at their expected values. (The fractal dimension D is equal to the reciprocal of the molecular weight exponent.) The static light scattering results for polystyrene in toluene (good) and cyclohexane (theta) solutions exhibited close to the expected fractal dimensions for mass scaling: $D = 1.63$ for solutions with excluded volume (theory predicts 1.67 - 1.70) and $D = 1.95$ for theta solutions (theoretical value is 2.0). The relaxation rate in the intermediate scattering regime is expected to scale as q^3. Experimental values of the exponent from light scattering experiments are typically about 2.8, however, by extending the scattering regime to higher values of qR, the authors were able to obtain a value of the exponent equal to 3.00 in a good solvent, and 2.88 in the theta solvent (because the radius of gyration is so much smaller in the theta solvent, the higher values of qR were not attainable, and thus the value of the exponent is lower in the theta solvent.) The shape of the dynamic structure factor was investigated by observing the large qR, long-time limit of the autocorrelation function, which is expected to behave as a stretched exponential decay, $\exp[(-t/\tau)^b]$, with the exponent b equal to 2/3 for good and theta solutions. Values of b equal to 0.72 and 0.71 for good and theta solutions, respectively, were obtained experimentally. The authors comment that other workers analyzing the stretched exponential behavior compared their data to a fit with b=2/3, rather than extrapolating an exponent directly from the data.

3.3.2. Semi-flexible and Rigid Polymers

Cotts [18] reported on the dilute solution characterization of polyamic acids and esters, precursors to the generally intractable polyimides. Condensation of pyromellitic dianhydride (PMDA) and oxydianiline (ODA) forms the polyamic acid PMDA/ODA, which upon cyclodehydration yields the corresponding polyamide. This polymer was analyzed by dilute solution viscometry, static and dynamic light scattering and SEC/LS in N-methyl pyrrolidone (NMP) solution. Electrostatic effects were observed in the viscometry and light scattering

results, but purification of the solvent eliminated these results, and normal dilute solution behavior was observed. The effects were attributed to amine impurities in the solvent which ionized the polymer. Equilibrium and exchange reactions due to the reversibility of the amine-anhydride condensation reaction were also found to complicate the polymer analysis. Attempts to synthesize polymer molecular weights higher than those predicted from the stoichiometry of the step-growth kinetics were initially successful, but after time, the lower equilibrium molecular weight was reached. This behavior was also observed for blends of differing molecular weights: a mixture of two molecular weights of biphenyl dianhydride/ODA over a period of two weeks reached an equilibrium molecular weight. Intrinsic viscosity measurements were made on polyamic acid solutions in NMP and the Mark-Houwink-Sakurada exponents "a" were found to range from 0.66 to 0.84. For low molecular weight semi-flexible polymers such as these, excluded volume effects are considered to be minimal, and thus the exponent > 0.5 is primarily attributed to the rigidity of the polymers. The translational diffusion coefficient from dynamic light scattering was measured for PMDA/ODA, from which a persistence length was calculated based on a theory for translational diffusion of wormlike chains. The value of 3.2 nm agreed well with estimates from the intrinsic viscosity data. The polymers studied were in general too low in molecular weight to obtain radius of gyration information from static light scattering - however one sample with a MW of 166K was analyzed by SEC/LS and an Rg/MW relationship was determined with an exponent of 0.59. In this case, the polymer was large enough that excluded volume contributions may be considered to be important in the molecular weight scaling exponent.

Dynamic light scattering of poly(gamma-benzyl-alpha, L-glutamate) (PBLG) in DMF solution was carried out at very low polymer concentrations by Jamil and Russo [19], and some unusual concentration dependencies were observed. A PBLG solution of molecular weight 280 000 showed an initial leveling off or decrease in the mutual diffusion coefficient with concentration for concentrations less than about 2 mg/ml. Above this concentration, a more pronounced increase in the diffusion coefficient with concentration was observed. Static light scattering measurements of PBLG at the low concentrations confirmed the absence of any aggregation that could cause the upturn in D_m. The parameter C which describes the q^2 dependence of the reduced first cumulant (Γ/q^2), can be analyzed if $qR_g > 1$. (For a rod-like polymer such as PBLG, R_g is large even for the low molecular sample used in this study, however the maximum value of qR_g was only about 2.) C contains information about the chain stiffness and translational-rotational coupling, and was found to decrease with increasing concentration. A low concentration limiting value of C was found to be ~ 0.1, which is the theoretical value for a monodisperse rodlike polymer with no translational-rotational coupling. The effect of translational-rotational coupling is to lower C while polydispersity effects and chain flexibility both raise C. Attempts to use DLS to estimate a MWD and thus the polydispersity of the polymer were marginally successful. Three DLS data analysis routines indicated bimodal character in the DLS data (although a rigorous test for bimodal character failed to confirm this), with a major molecular weight species M = 301 000 and a minor lower molecular weight component of M = 76 000 which gave a calculated weight average MW very close to the static LS results. Attempts to calculate a persistence length for PBLG based on measured and simulated values of C were very sensitive to polydispersity and the type of data analysis used.

Dynamic light scattering was used by Shukla, et al. [20] to study the rotational (Θ) and translational (D) diffusion coefficients poly(γ-benzyl α,l-glutamate) (PBLG) in benzyl alcohol solution in the isotropic and gel phases. PBLG forms a thermoreversible gel at low temperatures, even for very dilute solutions. All experimental correlation functions were found to be multi-exponential and were fit with a double exponential algorithm. The two extracted relaxation times (T1 and T2) were fit to D and Θ via $T1 = q^2D$ and $T2 = T1+6\Theta$ (only valid for very dilute

solutions). Both relaxation times were found to be linear in q^2. D was found to decrease with decreasing temperature, very sharply near the gel point. D was linear with concentration at low concentrations, but Θ was found to have no concentration dependence. Scaling theories by Doi and Edwards predict that D will scale with $c^{0.56}$ for semidilute solutions, but the exponent determined experimentally was 0.2, implying there are probably orientational interactions due to the rod nature of the polymer. The self-diffusion coefficient was found to scale with $c^{-0.75}$, not -0.44 as predicted by Flory's theory for the osmotic compressibility - the discrepancy probably stems from coupling between the translational and rotational motion. At temperatures above the gel point, correlation functions were exponential and two diffusion coefficients were determined; as the temperature was lowered toward the gel point, a damped oscillatory correlation function was observed; and at temperatures well below the gelation temperature, the correlation function was flat (no time dependence). The oscillatory functions were attributed to a non-equilibrium mass flow during gelation. The time dependence of the scattered light intensity was measured for samples quenched to below the gel point, and the pattern observed was consistent with an aggregation process (diffusion controlled fibrillar formation), and not spinodal decomposition.

Wissenburg, et al. [21] published a preliminary study on the aggregation of different molecular weight samples of poly(γ-benzyl-L-glutamate) (PBLG) in 1,2-dichloroethane solution monitored by static and dynamic light scattering. PBLG is a semi-flexible polymer known to aggregate in many solvents. The authors propose that PBLG dimerizes head-to-tail as the solution concentration increases. Plots of inverse scattered light intensity vs. concentration exhibit a minimum which can be extrapolated to yield the unaggregated polymer molecular weight (M), but when the higher concentration linear portion of the plot is extrapolated to zero concentration, apparent molecular weights are measured which have a ratio of M_{app}/M approximately equal to 1.7 (consistent with an equilibrium between monomers and dimers). In the same manner, apparent second virial coefficients are obtained from the static light scattering results, and the values obtained are reasonable for a head-to-tail dimer, and not consistent with a sideways dimer. Diffusion coefficients determined from dynamic light scattering experiments plotted against solution concentration yielded similar plots with minima which were deeper and shifted to lower concentration as the molecular weight of the sample increased. The initial decrease of the diffusion coefficient is probably due to a lengthening of the rod. Slopes obtained from linear plots of the diffusion coefficient vs. q^2 (q is the wave vector) were plotted as a function of solution concentration, and this time a maximum was observed, at roughly the same concentration as the minima were observed in the intensity and diffusion coefficient plots. This behavior is consistent with a theory proposed by Doi and others for head-to-tail aggregation - sideways aggregation is expected to lead to a plot in which the slopes decrease monotonically.

3.4. Copolymers and Polymer Mixtures

Dynamic light scattering of a mixture of two interacting polymers in a solvent which is thermodynamically good for both polymers is expected to exhibit two relaxations: the fast mode describing cooperative diffusion, and a slow mode attributed to an exchange or interdiffusion process. Daivis, et al. [22] investigated the ternary system polystyrene-poly(vinyl methyl ether)-toluene to determine the conditions under which the amplitude of the fast mode can be made negligibly small, and thus the slow mode can be equated to the self-diffusion coefficient of one of the polymers. The theory of ternary polymer solutions proposed by Benmouna and Borsali predicts that if one of the polymers is "invisible" (isorefractive with the solvent, such as PVME/toluene), and the ratio of the concentration of the visible polymer to the total polymer concentration, x, is small, the amplitude of the fast mode approaches zero. However, the theory also predicts that for a small χ/v ratio, where χ is the Flory interaction parameter for the two polymers, and v is the excluded volume (assumed the same value for both polymers), then the amplitude of the fast mode should vanish, regardless of the value of x. Daivis, et al. studied a

series of PS-PVME mixtures (of approximately equal molar masses) with x ranging from 0.001 to 0.246, and total polymer concentration up to 0.4 volume fraction, and found no evidence for a fast mode relaxation. Pulsed gradient spin echo (PGSE) proton NMR measurements on the same solutions used in DLS were performed to confirm that only D_S of the PS was being measured. The NMR spectrum of the PS-PVME-toluene system showed clearly separate regions for aromatic and aliphatic protons - thus the PS peaks were separate from the PVME, and D_S of the PS alone could be measured. (Toluene also had resonances in the aromatic region, but when the field gradient was applied, the different diffusion rates of the PS and the solvent led to a rapid attenuation of the solvent signal - also for some samples, deuterated toluene was used.) The self-diffusion coefficients of PS measured in this ternary system agreed with others in the literature for PS in other solvents. This confirms that the chemical differences between PS and PVME have little effect on the polymer diffusion, and that χ is small for the PS-PVME pair.

Giebel and coworkers [23] carried out dynamic light scattering measurements on mixtures of polydimethylsiloxane (PDMS) and polymethylmethacrylate (PMMA) in three different solvents (THF, toluene and chloroform), keeping the total polymer concentration constant while varying the polymer composition. Mixtures of two polymers exhibit two relaxations in solution - fluctuations of the total polymer concentration characterized by a cooperative diffusion coefficient, D_C, and an interdiffusive mode, D_I, which represents the relaxation of the composition fluctuations. As expected, D_C was found to be invariant with polymer composition over the entire composition range in all three solvents, and D_I followed an expected parabolic behavior over the same composition range. The three solvents were chosen because THF is isorefractive with PDMS, toluene is isorefractive with PMMA, and chloroform has a refractive index intermediate between those of the two polymers, and therefore when used as a solvent exhibits an effect called the "zero average contrast" (ZAC) in which the cooperative diffusion mode in DLS vanishes when the polymer composition $x = 0.5$ (the refractive index of the solvent matches the average refractive index of the polymer mixture). This ZAC condition was observed in chloroform solution by noting a change from a bimodal relaxation distribution to a unimodal distribution when x approached 0.5. Unimodal behavior was actually observed over a broader composition range ($x = 0.4$ to 0.6).

Haida, et al. [24] studied the semidilute solution properties of a polystyrene poly(methyl methacrylate) diblock copolymer in toluene solution via static and dynamic light scattering. The theory for diblock copolymers in a semidilute solution of a non-selective solvent predicts that two relaxations should appear in the DLS spectrum: the fast cooperative mode of the entangled network (the same as in homopolymer systems) and a structural mode which characterizes the motion of one chemical species with respect to the other. This structural mode should be observed in the zero average contrast condition (refractive index of the solvent matches the average refractive index of the copolymer) when no other modes are observed. Indeed, two relaxations in the DLS spectrum of the copolymer were experimentally observed: a fast mode corresponding to the cooperative diffusion of the network (also seen in a polystyrene homopolymer of the same molecular weight) and a slow mode. The slow mode apparently is not the expected structural mode because calculations based on the original theory predict that the structural mode should occur at a higher frequency than the cooperative mode, and the frequency of the observed slow mode extrapolates to zero at zero scattering angle (contrary to the theory). This observed slow mode is attributed to diffusion of large clusters which apparently form as the concentration exceeds the overlap concentration. The authors suggest that perhaps the structural mode has a small amplitude and is hidden behind the two more predominant relaxations.

Kent, et al. [25] published an extensive paper on the solution properties of polymer mixtures, employing static and dynamic light scattering as well as viscometry to study polystyrene (PS) as a dilute probe molecule in a solvent consisting of a poly(methyl methacrylate) matrix and a small molecule solvent. Toluene and ethyl benzoate were used as solvents (good solvents for both

polymers) and the concentration range employed covers the dilute and semidilute regimes. The focus of the paper is on the effects of χ_{PM} (where P denotes probe and M matrix polymers), which is small and positive, and the ratio of probe and matrix molecular weights. Static light scattering measurements of a PS probe (M_P = 900 000) in the presence of three molecular weights of PMMA matrix (M_M = 1 300 000, 70 000, and 7 000) were carried out to study the contraction of the probe polymer under various conditions. Scaling theories predict that for similar M_P and M_M, little interpenetration of polymer coils occurs until the overlap concentration is reached, which is the same for both polymers. However, when $M_P >> M_M$, the matrix polymers penetrate the coils of the larger probe molecules at all concentrations, and the matrix polymers act as a viscous solvent for the probe polymer, the concentration of the matrix polymer having little effect on the size of the probe molecule until the matrix overlap concentration is reached. The LS results for the largest and smallest matrix polymers employed in this study followed the scaling theory predictions, but the medium molecular weight matrix study yielded results which were inconsistent with either theory. The authors interpreted that study as one in which $M_P > M_M$, but M_P is not large enough to allow penetration by the matrix polymers. In this intermediate case, contraction of the probe is not observed until c_M exceeds the overlap concentration of the probe, c_P^*. Dynamic light scattering measurements were carried out to determine the dependence of the mutual diffusion coefficient (D_{PP}) on the concentration of the probe as a function of the matrix polymer concentration. With no matrix polymer present, the slope of D_{PP} vs. probe concentration was large and positive, because of large second virial coefficient (good solvent). As the concentration of the matrix is increased, the slope decreased and eventually becomes negative, due to the decreasing solvent quality. In conclusion, the authors found that the most significant effect of a matrix polymer is to alter the thermodynamic environment of the probe polymer, and the compatibility of the two polymers (χ_{PM}) is of secondary importance.

Seery, et al. [26] report on the dynamics of a copolymer containing predominantly polyacrylamide with a small amount (0.007 - 0.7 mol %) of a fluorocarbon-containing acrylate comonomer, which exhibits unusually large viscosity enhancements at low concentrations. The fluorocarbon nature of the hydrophobic portion of the polymer is apparently responsible for the large viscosity changes, since similar copolymers with a hydrocarbon hydrophobe required 1 to 2 orders of magnitude higher concentrations of the comonomer to exhibit similar viscosity changes. Static and dynamic light scattering measurements were used to investigate the molecular basis for the copolymer's high viscosities. At very low polymer concentrations, a large degree of polydispersity of hydrodynamic radii was found (DLS), indicating large clusters of associating polymers as well as small radii characteristic of collapsed chains. The aggregates appear to become more dense as the concentration of polymer is increased. A pseudo-gel mode was never attained (as seen by a fast and slow relaxations in the DLS spectrum), even after the estimated overlap concentration was exceeded. This is explained by clusters combining to form fewer more dense clusters, such that the number of clusters decreases, even when the number of chains added to the system increases. Addition of a surfactant with a sterically equivalent hydrophobe suppressed aggregation of the copolymer solutions, as evidenced by a single relaxation in the DLS spectrum.

3.5. Polyelectrolytes

Amis and Hodgson [27] reported on the DLS and viscosity of linear and cyclic poly(2-vinyl pyridine) in ethylene glycol solution with two different concentrations of HCl added to protonate the pyridine group. The focus of this paper was to compare properties of linear and ring polyelectrolytes of the same molecular weight, and to compare the ratios of the properties (cyclic/linear) with those previously reported for neutral polymers. DLS and intrinsic viscosities at high concentrations of added salt (where electrostatic interactions are more screened) exhibited

normal polymer behavior. At low ionic strength, a maximum was observed in the plot of the reduced viscosity vs. polymer concentration, reflecting the polymer size changes on dilution. The concentration at which the maximum viscosity occurred was independent of chain topology, although the cyclic polymers appeared to undergo a larger electrostatic expansion than the corresponding linear polymers

An investigation of the electrostatic persistence length (l_{pe}) of a flexible polyelectrolyte, poly(2-vinylpyridiniumbenzyl bromide), as a function of solution ionic strength was carried out by Forster, et al. [28] using static and dynamic light scattering. The current theory for polyelectrolyte solutions developed by Skolnick, Fixman, and Odjik (SFO) in the 1970's predicts an inverse ionic strength dependence of the electrostatic persistence length, which has generally not been proven experimentall The authors numerically evaluated an older theory (1950's) of Kuhn, Katchalsky, and Lifson using a wormlike chain segment distribution instead of the Gaussian distribution originally proposed, and their calculations predict a chain length dependent l_{pe}, with a weak ionic strength dependence which does not follow a simple scaling law. The authors restricted the polyelectrolyte and added salt concentrations for the light scattering studies to avoid the problems associated with intermolecularly interacting polyions at low polyion concentration, and the "extraordinary phase" of polyelectrolyte solutions observed when the molar polyion concentration exceeds the molar salt concentration. The authors believe the inclusion of these complicating factors in previous light scattering studies is one reason for the large discrepancy among published experimental polyelectrolyte results. Static and dynamic light scattering were used to analyze two polymer samples of molecular weights 372 000 (A) and 940 000 (B), which were quarternized to 100% and 69%, respectively. The electrostatic persistence lengths evaluated from R_g values (SLS) were consistently higher than those obtained from DLS (R_h measurements), and there was a very slight chain length dependence observed only from the dynamic measurements. The experimental results qualitatively matched the numerical calculations very well, the latter being larger by a factor of approximately two, although the chain length dependence was not observed.

Peitzsch and coworkers [29] initiated a light scattering study to determine the draining characteristics of linear polyelectrolytes, specifically, the biological polymers heparin (Hep) and chondroitin 6-sulfate (ChS), and a synthetic polyelectrolyte, sodium poly(styrene sulfonate), NaPSS. The three hydrodynamic regimes discussed include free-draining, in which the diffusion coefficient, D_O, has an inverse linear relationship with the molecular weight (i.e., independent of radius of gyration, Rg, and hence the ionic strength, C_S); non-draining, in which D_O scales as M to the power of -0.5, and thus is a measure of the static size of the polymer, R_g; and partial-draining, which is intermediate in behavior between the two extremes. From dynamic light scattering, D_O for Hep and ChS were found to be independent of C_S, over a large range of C_S studied. Since the radius of gyration is expected to vary with the ionic strength (due to shielding effects of the counterions), the authors conclude that the polymers exhibit at least partial draining behavior. NaPSS exhibited the same behavior for low C_S, but for C_S greater than 30 mM, there was a marked dependence of D_O on the ionic strength. The authors cautiously conclude that at low ionic strength, NaPSS is free-draining, at intermediate ionic strength, it exhibits partial draining behavior, and at high ionic strength, non-draining (or least draining) behavior is observed. The bulkier side-groups of NaPSS could explain the difference between the non-draining behavior of NaPSS at high ionic strength vs. the draining condition observed at all C_S for the biological polymers. The use of dynamic light scattering as a sizing technique necessitates the correlation of R_h (measured by DLS) with R_g, the actual polymer size. Thus ascertaining the draining characteristics of polymers is important, especially in the case of polyelectrolytes, whose static sizes vary a great deal depending on the solvent environment.

Sedlak and Amis published two papers dealing with the dynamics of salt-free polyelectrolyte solutions - the first [30] of these papers deals with the molecular weight dependence of the solutions. A series of sodium poly(styrene sulfonate) (NaPSS) samples ranging in molecular weight from 5K to 1200K were studied in the concentration range 10 - 46 g/L in aqueous

solution. When the added salt concentration is decreased in polyelectrolyte solutions, at some critical salt concentration, the autocorrelation function splits into two exponentials - this is called the "extraordinary phase" in polyelectrolyte solutions. The fast diffusion coefficient is attributed to coupled diffusion of the polyions and counterions, and was found experimentally to be independent of molecular weight over several decades of MW, and nearly independent of concentration for a given MW. This implies that the coupling of the polyion/counterion motion is dominated by counterion fluctuations and is little influenced by polymer hydrodynamic behavior. The slow mode has been described as the diffusion of multi-chain clusters. The size of these clusters remains relatively constant at a given concentration for molecular weights < 70K, and then increases slightly with an increase in molecular weight. Because of the large size of the clusters, the scattering wave vector responsible for the slow mode fluctuations is not strictly due to translational diffusion, but also contains contributions due to internal motions. In general, counterions are very important for both the dynamics of the individual polymer molecules and the domains (clusters).

The second [31] paper of Sedlak and Amis proposes a concentration-molecular weight diagram describing the different dynamical regimes using static and dynamic light scattering. This paper extends the concentration range of the first paper to include very dilute solutions for three molecular weight NaPSS samples - 5K, 100K, and 1200K. Three different concentration regimes were observed - Regime I corresponds to the most concentrated solutions (0.5 - 50 g/L) and is independent of molecular weight. This regime is characterized by formation of large chain clusters and a strong coupling of the polyion and counterion diffusion, as observed by the angular dependencies of the scattering intensity and the slow diffusion coefficient, and a strong concentration dependence of the scattering intensity. Regime II is the intermediate concentration regime (0.001 - 0.5 g/L) where strong repulsive interactions between polyions are observed as a weak concentration dependence of the total scattering intensity. Regime III is the very dilute regime where polyions are separated by large distances, and intermolecular attractions are weak, and thus a concentration-independent angular dependence of the scattering intensity is observed. Regime II is separated from regime III by a concentration of 0.001 g/L, but the very dilute behavior has only been observed for high molecular weights, so the line only extends to a molecular weight of 300K. A line describing the theoretical transition from dilute to semidilute behavior has been drawn diagonally through regimes I and II, although the authors did not observe this transition experimentally. The equation used to calculate the crossover concentration (dilute to semidilute transition) does not take any repulsive or attractive intermolecular interactions or the role of the counterions into consideration which is extremely important in the case of salt-free polyelectrolyte solutions.

3.5.1. Polyelectrolyte Complexes

Nonstoichiometric polyelectrolyte complexes (NPEC) formed by the reaction of poly(acrylic acid) (or poly(methacrylic acid)) with alkyltrimethylammonium bromides (where the alkyl moiety is a dodecyl, tridecyl or cetyl group) were studied by Ibragimova, et al. [32] using static and dynamic light scattering. Most reactions between micelle-forming surfactants and oppositely charged polyelectrolytes form products insoluble in water, however, the authors found that the aforementioned NPECs were soluble in water with the addition of a simple salt. Above a certain solution concentration (varies depending on the exact complex studied), the polycomplexes do not dissociate, and the concentration of the free surfactant (SA) ions was determined to be less than 10^{-5} mol/l. The composition of the complex is described by ϕ, the ratio of the number of SA ions to the number of repeat units of the polymer in the complex. From static light scattering measurements, all NPEC particles were found to contain a single polyelectrolyte chain, and the molecular weight of the complex increased linearly with ϕ. This implies a uniform distribution of the SA ions about the complex (as opposed to a nonuniform distribution where the measured M_W would be the average of a fully occupied (by SA ions) complex and a linear polyelectrolyte

with no anions.) The second virial coefficient, A_2, decreased with increasing ϕ, as a result of the decrease in charge of the polyanion as SA ions neutralize the carboxyl groups. From dynamic light scattering studies, the hydrodynamic radii of the NPEC remained constant or increased with increasing ϕ. This is in contrast to behavior observed for "polysoaps" (copolymers with covalently bound hydrophobic as well as hydrophilic groups), in which the hydrodynamic radii decrease with an increase in the hydrophobic group content. This discrepancy can be rationalized by realizing the only way for a polymer with covalently bound hydrophobic groups to minimize contact with the solvent is to become more compact. On the other hand, the ionic bonds of the SA ions are more flexible, and can migrate along the chain, allowing for more conformational variations in which the hydrophobic groups can associate.

Complex formation between poly(ethylene oxide), PEO, and lithium (and sodium) dodecyl sulfate micelles, LDS and SDS, was studied by Xia, et al. [33] using light scattering (static, dynamic and electrophoretic) and dialysis equilibrium studies. Although this polymer complex has been studied for over 20 years, the nature of the stabilizing interactions between the micelles and the polymer in the complex have not been adequately addressed - this study is an attempt to systematically vary the polymer molecular weight; polymer, surfactant, and added salt concentrations; and to test a hypothesis previously proposed by the authors regarding the role of the cation in the polymer-micelle interactions. The molecular weight of the of the PEO employed was 145K, except for studies on the effects of molecular weight in which M ranged from 25K to 996K. Total intensity light scattering was measured as a function of surfactant concentration for different ionic strengths. The intensity rapidly increased initially and then leveled off with LDS concentration, corresponding to saturation of the complex. The scattering intensity of the saturated complex increases with ionic strength presumably due to shielding of the electrostatic repulsions between polymer-bound LDS micelles. Consistent with these results, dialysis equilibrium studies found that the number of bound micelles increased with increasing ionic strength. DLS was measured for all molecular weight samples for a series of surfactant concentrations, and the distribution of relaxation times changed from a single relaxation mode at low LDS concentrations (due to unsaturated polymer complexes), to two relaxations at higher concentrations, caused by the appearance of free LDS micelles and saturated polymer complexes. The molecular weight dependence of the diffusion coefficient for PEO complexes and surfactant-free PEO were both linear, with molecular weight scaling exponents of -0.55 and -0.52, respectively, indicating both are good solvent systems. The electrophoretic mobilities of the PEO-LDS complexes were found to be nearly independent of molecular weight, corresponding to a free draining coil, typical polyelectrolyte behavior. As a result of this study and a previous one investigating the effects of different cations on the critical micelle concentration in PEO, the authors propose that the cation of the surfactant coordinates with the polymer forming a "pseudopolycation" which then electrostatically interacts with the surfactant anionic micelles.

3.6. Micelle-forming Polymers

Static and dynamic light scattering were used to study the interactions between poly(ethylene oxide) and the ionic surfactant sodium dodecyl sulfate (SDS) in aqueous solution by Brown, et al. [34]. At low concentrations of SDS, solutions of PEO and SDS contain mostly free SDS, but as the concentration of SDS increases, the critical aggregation concentration (cac) is reached, and most of the SDS is bound in the form of micelles to the polymer chain. The purpose of this light scattering study was threefold: (1) to demonstrate that during the formation of the charged complex, polyelectrolyte character is imparted to the neutral PEO chain; (2) to elucidate the composition of the charged complex in the presence of added NaCl; and (3) to investigate the modification of the polyelectrolyte properties when excess SDS is added. Intrinsic viscosity and static light scattering measurements indicated a large coil expansion with a decrease in the added salt concentration for a fixed ratio of SDS/PEO, typical polyelectrolyte behavior. A maximum in the hydrodynamic radius (determined from DLS) was obtained for the ratio of SDS/PEO of ~5

(for a given PEO concentration) indicating saturation of the binding of SDS with PEO - above this concentration of SDS, the radius decreases due to screening effects from the counterions of the excess SDS. Relaxation time distributions from dynamic light scattering showed separate peaks due to charged polymer complexes and the smaller free SDS micelles. The position (i.e., size of particle) and intensity of these peaks varied depending on the concentrations of the polymer, SDS and the added salt. Temperature effects were not measured.

The effects of relative block sizes on the aggregation properties of triblock copolymers in aqueous solution was studied by Brown, et al. [35] using static and dynamic light scattering, intrinsic viscosity and oscillatory shear measurements. The copolymers analyzed all had a central block of 39 propylene oxide units flanked with varying lengths (6, 67 and 96 units) of ethylene oxide endblocks. Typically, at the lower temperatures, monomers (single polymers) and clusters of polymers were present, and as the temperature increased, micelle formation was observed (as an intermediate size particle in the DLS spectrum). If a high enough temperature could be reached before the solution clouded, micelles became the predominant species. The copolymer with the shortest PEO block exhibited only monomer and cluster formation in solution (because its cloud point was quite low), but the other two copolymers simultaneously formed micelles, monomers and clusters at certain temperatures and polymer concentrations. Physical gelation occurred from overlap of micelles at a well-defined temperature for a given concentration, and dynamic screening lengths were determined from the cooperative diffusion coefficients measured under those conditions. Gels were found to be more stable the longer the PEO endblock, probably due to a higher entanglement of the PEO chains in the mantle of the micelles. The inverse osmotic compressibility, $\partial\pi/\partial c$, (related to the second virial coefficient) was determined from static light scattering and correlated to the formation of clusters and micelles. Typically, low values of $\partial\pi/\partial c$ favored formation of clusters and micelles.

Chu [36] describes the conformation and dynamics of colloidal aggregates in detergent and copolymer systems using laser light scattering, X-ray scattering, and rheological measurements. Cobalt monooleate, $Co(OH)(C_{17}H_{33}COO)$, can form bridges between the cobalt atoms and the hydroxy groups in non-polar solvents, and thus forms long aggregated complexes with -(Co-O(H)-Co)- as the backbone. Viscosity measurements of a 0.7% cobalt monooleate benzene solution indicated three different flow regions - at low shear rates, Newtonian flow of very high viscosity was observed, indicating a semidilute solution, due to the long chains formed during aggregation. Shear thinning was observed at intermediate shear rates, probably caused by alignment of the chains, and subsequent breakup of the aggregates. At high shear rates, the viscosity is similar to the solvent viscosity, attributed to the breakup of most of the aggregates. Block copolymers of polystyrene and poly(isoprene) were found to form micelles and vesicles (hollow spheres with a solvent core) in aniline solution (aniline is isorefractive and has isoelectron density with PS as well as being a selective solvent for PS, which makes the light and X-ray scattering experiments easier.) Formation of vesicles over micelles was favored when the PS/PIP blocks were similar in size. DLS and SAXS were used to determine the hydrodynamic radii of the supramolecular particles, the core radii and to distinguish between the two types of supramolecular formation. Triblock copolymers of poly(oxyethylene oxypropylene oxyethylene) were also studied, since they form micelles with a PPO core in water. They can also form reverse micelles in *o*-xylene. In *o*-xylene solution, small amounts of water may be solubilized in the PEO core. DLS was used to measure the increase in hydrodynamic radius of the micelles as the concentration of added water was increased.

Micellization and gelation properties of stat-copoly(oxyethylene-oxypropylene)-block-poly(oxyethylene) in aqueous solution were studied by Deng, et al. [37] via static and dynamic light scattering, surface tension and electron microscopy. Block copolymers of E/P (oxyethylene and oxypropylene) with long P blocks are very hydrophobic, and have very low critical micelle concentrations (cmc's) - substitution of a statistical E/P block for the P block allows control over

the hydrophobicity of the copolymer by adjusting the E/P ratio in the statistical block. The critical micelle temperature (cmT) was determined for a series of copolymers at different solution concentrations by monitoring the light scattering intensity as the temperature of the solution was incrementally raised. The LS intensity below the cmT is constant (solution of unimers), increases at the cmT, levels off again (solution of micelles) and then dramatically increases as the cloud point is reached. Alternatively, cmc's were determined by measuring the LS intensity at a given temperature for different concentrations above and below the cmc. The results from the two experiments overlapped. The cmT's determined in this manner were dependent on the solution concentration, but the effect was not as dramatic as changing the composition of the statistical block. Dynamic light scattering was used to determine the size of micelles (R_h), and hydrodynamic radii were found to be consistent among different copolymer samples (~15 nm), but certain samples had very large R_h (50-80 nm) suggestive of micelle aggregation. Static LS was used to measure micellar molecular weights, which were ~200 000 for the unaggregated micelles, and > 1 x 10^6 for the aggregated micelles. Electron microscopy confirmed the micelles were of spherical shape and uniform size distribution. The thermodynamics of micellization were analyzed from plots of $(cmT)^{-1}$ vs. log c. At a constant temperature, decreasing the P content of the statistical block or increasing the length of the E block increase the free energy of micellization. Thermally reversible gelation was observed for concentrated solutions of block copolymers, in solutions that formed micelles. Micellar solutions were found to solubilize a related statistical copolymer (no ethylene block) under certain conditions.

Ionomers which form reverse micelles (hydrophilic core, hydrophobic shell in organic solvent) were studied by Desjardins, et al. [38] via dynamic light scattering and viscometry, and compared with earlier studies on the same polymers using size exclusion chromatography. The ionomers studied were block copolymers of styrene with either methacrylic acid or a metal methacrylate ester, where the metal was sodium or cesium, and the methacrylic group was always less than 4 percent of the copolymer. The neutralized copolymers formed micellar solutions in any solvent which dissolves polystyrene (PS), however the acid copolymers only formed micellar solutions in aprotic solvents in which PS is soluble, i.e., CCl_4, toluene, cyclohexane. The neutralized polymers were found to form micelles of similar hydrodynamic radii (R_h) in solvent with similar affinities for the PS shell (as determined from the Mark-Houwink exponents). However, DMF which has a lower affinity for PS than CCl_4, has a smaller r_h, as might be expected, but independent measurements of micellar molecular weights indicated that micelles in DMF have a lower aggregation number which might also be a factor in their smaller size. Since DMF has a higher affinity for the ionic cores, more solvent is present in the core, which plasticizes the polymer, thereby reducing the T_g and allowing the micelles to reorganize into thermodynamically more favorable smaller micelles. The effects of solution preparation on the size of micelles was also investigated. Sodium and cesium micellar solutions were typically prepared by freeze drying the solution in which the acid polymers were neutralized and after thorough drying of the polymer powder, subsequent dissolution in the desired solvent. The acid micellar solutions were prepared by dissolving the copolymers in THF (molecular solutions) and casting films which were dried, and subsequently dissolved in the appropriate solvent. The r_h's of the micelles prepared from the dried forms of the acid and neutralized polymers were compared with the radii of the micelles formed directly in solution, and for both types of polymers the dried forms of the polymers produced significantly larger micelles. The nature of the solvent used for the neutralization reaction, also affected the size of the final micelles. Both acid and neutralized micelles were found to be stable in solution for several days, and there was no indication of a micelle-single chain equilibrium.

Richtering, et al. [39] studied a non-ionic polymeric surfactant in aqueous and organic (methanol) solutions using static and dynamic light scattering and compared the properties with those of the corresponding monomer (which forms micelles) in aqueous solution. The surfactant

in this study is a poly(ethylene glycol) monoalkylether, $(CH_2)_{11}(OCH_2CH_2)_8OCH_3$, with a methacrylate group attached to the alkyl end. The methacrylate group is then polymerized to form a poly(methacrylate) with pendant amphiphilic surfactant groups. Two polymer samples, designated 1 and 2, of MW's 620K and 290K, respectively, were studied. In methanol, both samples showed normal dilute and semidilute solution behavior for flexible linear polymers, although the solvent was not as thermodynamically good for the second sample. In aqueous solution, the two polymers exhibited different behavior from the aqueous monomeric surfactant solutions, and more surprisingly, also from one another. In dilute aqueous solution, static light scattering indicated that the first sample formed aggregates of approximately two polymers at concentrations greater than 2 g/L. The second sample did not form aggregates, however a theta temperature was observed at 30 C, from which the characteristic ratio of the polymer was determined to be 54, which is much larger than that of PMMA (8) and poly(hexadecyl methacrylate) (25). Hydration of the ethylene glycol groups may make the side chain appear more bulky than a simple alkyl group. Intrinsic viscosity and DLS studies indicate partial draining character for the polymer, and an estimate of the draining parameter h=0.35 was made. The monomer forms micelles of approximate molecular weight 44K, much smaller than either of the polymer molecular weights, and are more densely packed. When the degree of polymerization of the polymer micelle exceeds the aggregation number of the surfactant, nonsaturated sites on the polymer become available and lead to aggregation of the polymers. This occurs in the first sample, but not the second, the cause of which may be related to a difference in tacticity between the different samples.

Equilibrium effects of micelles formed from polystyrene-block-poly(ethylene-co-propylene), PS-PEP, in the solvents decane and diisopropylether (DIPE) were investigated via static and dynamic light scattering, small-angle X-ray scattering (SAXS), viscometry and differential scanning calorimetry by Stejskal, et al. [40]. Unusual properties were observed for PS-PEP micelles in decane solution: (1) very large molecular weight micelles were detected via static and dynamic LS and SAXS (30-60 million), which upon heating to 100 C and subsequent cooling were reduced to more reasonable values of (8-15 million); (2) higher viscosities were observed in decane solution than in a nonselective solvent and the viscosity increased following the heat treatment (micellar solutions should exhibit a lower viscosity than the corresponding unimer solution); (3) static LS showed dissymmetries of scattered light (ratio of scattered light intensities at 45^o and 135^o) of less than unity for native (unheated) and heat treated solutions, usually indicative of interparticle interactions; and (4) the correlation functions from dynamic LS were not single-exponential in character (suggestive of non-uniform micelles), however, SAXS data indicated monodisperse character. PS-PEP also forms micelles in DIPE, however normal micellar behavior was observed in this solvent (micelles similar in size to the heat treated decane solution are formed.) The authors conclude that the decane solutions maintain their solid state structure when initially dissolved (solid state SAXS data confirms this) because the PS core remains frozen due to unfavorable interactions with the solvent (DIPE is a better solvent for PS than decane); after heating above the glass transition, the micelles reorganize themselves into equilibrium micelles. The static and dynamic light scattering and viscosity results are indicative of attractive interactions among micelles, even though decane is a good solvent for the PEP micellar shell (polyolefins have been known to associate in hydrocarbon solvents). These "sticky contacts" are operative when the micelles are in close proximity (the authors observed these interaction phenomena to increase with increasing polymer concentration) and could lead to gelation. No interactions were observed for DIPE micellar solutions.

The micellization of di- and triblock polystyrene-poly(ethylene oxide) copolymers in water was studied by Xu, et al.[41], using static and dynamic light scattering to quantitatively test the star and mean-field models of micellization. The star model of micellization is derived from predictions of star polymers, and uses scaling arguments about the dependence of N, the association number of the micelles, R_C, the core radius, and L, the corona thickness on the chain

lengths of the two copolymer constituents, N_A and N_B. This model is most useful for micelles that resemble star polymers: a small core with long chains protruding from the core. The mean field models are more appropriate for micelles with a large core and thin shell, and use mean-field approximations to predict values of N, R_c and L from known values of Flory-Huggins χ parameters. Even though these models differ in their theoretical approaches, predictions about micellar size are subtle, and unless copolymers with a great distribution of chain lengths are studied (not the case in this study), these differences may be indistinguishable. The copolymers studied ranged in MW from 100K to 7K, with weight fractions of PEO (component A) ranging from 89% to 26%, however, depending on the MW, only those copolymers with PEO content greater than 60 to 75% formed micellar solutions. The micelles were found to associate in solution, thereby complicating the LS analysis. The DLS data analysis yielded bimodal distributions for all solutions (indicative of micelles and micelle clusters) but the different radii were able to be resolved because the linewidths were separated by more than a factor of two. The R_h's determined in this manner were equivalent to the core radius predicted by the star model for 7 of the 9 samples studied. At this point, assuming the star model to be valid, the prediction for the aggregation number, N, was substituted into the molecular weight data analysis routine which led to a plot in which the experimentally determined M_w's for the di- and tri-block copolymers formed lines with a common intercept, but different slopes. This implies that both copolymer systems fit the star model but have slightly different structures. Once the values of N and R were determined from the star model, these values were used to predict the parameters $\chi_{PS\text{-}PEO}$ and $\chi_{PEO\text{-}water}$, which agreed well with values in the literature (since the core is considered to be solvent-free, $\chi_{PS\text{-}water}$ can be neglected.) Thus, aspects of both theories of micellization were confirmed by this study.

3.7. Semidilute Solutions and Gels

Fang, et al. [42] examined the effects of solvent quality on the static and dynamic properties of polyacrylamide solutions and gels by varying the composition of a mixed solvent containing water and glycerol (PAA gels were prepared by cross-linking with bisacrylamide). Since the effect of changing the solvent composition is similar to changing the temperature in a single solvent (because the theta temperature shifts as the solvent composition changes), the effects of temperature on these properties can also be studied. The authors compared experimentally determined values of the longitudinal osmotic modulus, M_{OS}, the correlation length, ξ (static and dynamic), and the frictional coefficient, f, to values predicted by the mean-field (as interpreted by Tanaka for gels) and scaling theories. From static light scattering, the second virial coefficient was found to be linear with the solvent composition, and thus a scaling relationship between A_2 and the reduced temperature (deGenne) can be used to convert properties dependent on the solvent composition to a temperature dependence. The solutions and gels behaved qualitatively similar, with the scaling exponents varying slightly. Static properties were predicted more closely by scaling theory than the mean-field theory, and dynamic properties were too complex to be described by simple power laws. The viscosity of the glycerol/water mixture changes dramatically over the range of solvent composition (approx. 0 to 90 percent glycerol) , and this greatly complicated the frictional property analysis.

Konak and coworkers [43] published the fifth in a series of papers dealing with the dynamic properties of partially neutralized poly(methacrylic acid) solutions and gels. This paper deals specifically with the differences between fully neutralized PMA solutions and gels (the gels were prepared by copolymerizing sodium methacrylate with bisacrylamide). Three dynamic regimes (fast, medium and slow) were observed from the DLS analysis of the PMA solutions. The fast mode is attributed to the network cooperative diffusion mode, the medium mode is a consequence of the size polydispersity in the sample (verified by GPC measurements), and the

slow mode is characterized by slow fluctuations with large correlation length, probably due to the formation of clusters or domains. The gel samples gave a similar fast mode diffusion coefficient, but instead of a well resolved slow mode, a distribution of peaks was observed, attributed to diffusion of the sol in the gel. The time dependence of the gel autocorrelation functions follows a power law with an exponent of 0.25 to 0.30, in the range reported for the dynamics of interacting polymer clusters having percolation type mass distributions.

The thermoreversible gelation of ethyl hydroxyethyl cellulose (EHEC) in the presence of a surfactant (cetyltrimethylammonium bromide, CTAB) was studied in aqueous solution by Nystrom, et al. [44] via static and dynamic light scattering. In semidilute solution, binding of CTAB surfactant molecules to polymer chains is believed to create micelle-like aggregates which then are attracted to hydrophobic parts of other polymer chains and results in a physically cross-linked network. In dilute solution, static light scattering (SLS) was used to observe a coil expansion with increasing temperature, presumably due to increased binding of surfactant to polymer molecules, with a resultant electrostatic repulsion between the ionic micelles. In semidilute solution, SLS revealed a decrease in mesh size with increasing temperature, indicative of an increase in crosslink density as the temperature rises. Dynamic light scattering (DLS) studies were interpreted in light of a theory developed by Semenov for polymer dynamics in the entangled regime. This theory predicts that two relaxation modes will be observed in the correlation function: a fast cooperative mode in which the polymer chains are collectively moving relative to the solvent, and a slow reptation-like mode in which each chain is confined by its neighboring chains, and can only reptate in a snake-like fashion. The fast cooperative mode was observed and found to be relatively independent of temperature, i.e. not affected much by the gelation process, however the decay times of the slow mode were found to shift dramatically to longer times as the temperature increased. DLS experiments of semidilute EHEC solutions without surfactant did not show the characteristic long relaxation times associated with the gelation process, thus ascertaining the importance of the surfactant in the cross-linking process.

A bimodal polydimethylsiloxane (PDMS) network, prepared by end-linking two different molecular weight PDMS prepolymers (M_n ~ 2500 and 40,000), was studied via dynamic light scattering by Oikawa [45] to assess its structure. Several theories have been proposed to explain properties unique to bimodal networks, and this author believes a spatially and compositionally heterogeneous network accounts for the differences observed between unimodal and bimodal networks. The autocorrelation function was well fit by a double-exponential decay, with the fast mode attributed to cooperative diffusion of the network chains and a slow mode proposed to be due to self-diffusion of a certain size cluster. The two modes of relaxation are indicative of a heterogeneous network structure comprised of small and large mesh domains.

PDMS networks (swollen with toluene) and PDMS/toluene semidilute solutions were analyzed via DLS by Patel and Cohen[46]. Heterogeneous networks were prepared by end-linking difunctional PDMS with monofunctional PDMS and a tetrafunctional cross-linker to achieve networks with different sizes and number of pendant groups. The cooperative diffusion coefficient (fast mode observed in DLS) in the "fixed-solvent" frame of reference, D_c^S, for semidilute solutions and gels is predicted to scale with the concentration of the polymer to the powers of 0.75 and 1.0 for polymer solutions with and without excluded volume, respectively. (The equality between semidilute solutions and gels comes from the analogy that the solutions can be considered as gels whose crosslinks have finite lifetimes.) Experimentally, the exponent was determined to be 1.1 for networks and 0.97 for the semidilute solutions. Two explanations were offered for this discrepancy: first, toluene is not a particularly good solvent for PDMS, therefore the exponent may be closer to 1.0 than 0.75, and secondly the solutions probed in this study were more concentrated than the semidilute regime as defined by deGenne (volume fraction of polymer < 0.1). The ratio of the magnitude of the diffusion coefficient of the networks to the solutions was found to be independent of concentration, and equal to 1.45, in

good agreement with the prediction of 1.5 based on the Flory-Rehner model of highly swollen networks. No significant differences were observed in the dynamic behavior of networks with different topology.

Suzuki and coworkers [47] studied the formation of inhomogeneities in poly(acrylamide) (AA) and poly(N-isopropylacrylamide) (IPA) gels using dynamic light scattering. Both of these gels were formed by reacting the appropriate monomers with N,N'-methylenebisacrylamide (bis) as the cross-linking agent in aqueous solution. By changing the temperature of the gelation reaction, homogeneous (transparent) or inhomogeneous (opaque) gels can be formed. For AA gels, the homogeneous networks are formed at high gelation temperature, and for IPA gels, the homogenous structures are formed at low gelation temperature. By polymerizing four samples (two of each polymer sample, one at high and one at low temperatures), the heterogeneities of the two different gels were compared. The position dependence of the scattered light intensity was measured for the four gel samples, and the presence of inhomogeneities was confirmed by large spatial fluctuations of the scattered light intensities for the AA sample at low temperature, and the IPA sample at high temperature (the "homogeneous" gels were not really homogeneous but significantly more homogeneous than the "inhomogeneous" gels). DLS was also used to analyze the correlation functions of the solutions as they were undergoing gelation. For AA gels polymerized at high temperature, a single fast relaxation (attributed to cooperative diffusion of the network) was observed during the course of the reaction, behavior expected for an ideal gel. At low polymerization temperatures, however, an initial fast relaxation was observed, but as the reaction proceeded, another slower relaxation appeared and grew in intensity. Once the gelation reaction was complete, the slow relaxation disappeared, and thus it was surmised that this slower relaxation was related to diffusion of large clusters within the existing network. The reaction rate of bis monomers has been determined to be faster than that of AA monomers, and bis monomers are not as soluble at low temperatures; therefore the authors conclude that bis-rich clusters form early in the reaction, and at low temperatures are insoluble, and thus when the gelation is complete, these bis domains are frozen in the network, which results in an inhomogeneous gel. The same behavior at opposite temperatures was observed for the IPA gels. IPA linear polymer is insoluble at high temperature, and thus the formation of inhomogeneous IPA gels at high temperature may be caused by domains of IPA-rich polymers frozen into the network.

4. References

1. S. I. Ali, *J. Appl. Polym. Sci.: Appl. Polym. Sympos.* **1992,** 51, 293.
2. M. Bercea, S. Ioan, B. C. Simionescu, C. I. Simionescu, *Polym. Bull. (Berlin)* **1992,** 27,571.
3. S. R. Gooda, M. B. Huglin, *Macromolecules* **1992,** 25, 4215.
4. Y. Nakamura, K. Akasaka, K. Katayama, T. Norisuye, A. Teramoto, *Macromolecules* **1992,** 25, 1134.
5. A. M. Oun, *Polym. Int.*, **1992,** 29, 307.
6. T. Griebel, W. M. Kulicke, *Makromol. Chem.* **1992,** 193, 811.
7. D. Hunkeler, X. Y.Wu, A. E. Hamielec, *J. Appl. Polym. Sci.* **1992,** 46, 649.
8. H. Mattoussi, S. O'Donahue, F. E. Karasz, *Macromolecules* **1992,** 25, 743.
9. E. Nordmeier, W. Dauwe, *Polymer Journal (Tokyo)* **1992,** 24, 229.
10. L. Ould-Kaddour, C. Strazielle, *Polymer* **1992,** 33, 899.
11. J. R. Quintana, M. Villacampa, M. Munoz, A. Andrio, I. A. Katime, *Macromolecules* **1992,** 25, 3125.
12. J. R. Quintana, M. Villacampa, A. Andrio, M. Munoz, I. A. Katime, *Macromolecules* **1992,** 25, 3129.
13. B. R. White, G. J. Vancso, *Eur. Polym. J.* **1992,** 28, 699.
14. G. D. J. Phillies, W. Brown, P. Zhou, *Macromolecules*, **1992,** 25, 4948.
15. N. A. Rotstein, T. P. Lodge, *Macromolecules* **1992,** 25, 1316.

16. B. Li, Y. Yang, S. Ni, *J. Appl. Polym. Sci.*, **1992**, 46, 1691.
17. J. E. Martin, J. P. Wilcoxon, J. Odinek, *Macromolecules*, **1992**, 25, 4635.
18. P. M. Cotts, *J. Appl. Polym. Sci.: Appl. Polym. Symp.*, **1992**, 51, 101.
19. T. Jamil, P. S. Russo, *J. Chem. Phys.*, **1992**, 97, 2777.
20. P. Shukla, M. Muthukumar, K. H. Langley, *J. Appl. Polym. Sci.*, **1992**, 44, 2115.
21. P. Wissenburg, T. Odijk, M. Kuil, M. Mandel, *Polymer*, **1992**, 33, 5328.
22. P.J. Daivis, D. N. Pinder, P. T. Callaghan, *Macromolecules*, **1992**, 25, 170.
23. L. Giebel, R. Borsali, E. W. Fischer, M. Benmouna, *Macromolecules* **1992**, 25, 4378.
24. H. Haida, J. Lingelser, Y. Gallot, M. Duval, *Makromol. Chem.* **1991**, 192, 2701.
25. M. S. Kent, M. Tirrell, T. P. Lodge, *Macromolecules*, **1992**, 25, 5383.
26. T. A. P. Seery, M. Yassini, T. E. Hogen-Esch, E. J. Amis, *Macromolecules* **1992**, 25, 4784.
27. E. J. Amis, D. F. Hodgson, *Polymer Preprints* **1992**, 32, 617.
28. S. Forster, M. Schmidt, M. Antonietti, *J. Phys. Chem.*, **1992**, 96, 4008.
29. R. M. Peitzsch, M. J. Burt, W. F. Reed, *Macromolecules* **1992**, 25, 806.
30. M. Sedlak, E. J. Amis, *J. Chem. Phys.* **1992**, 96, 817.
31. M. Sedlak, E. J. Amis, *J. Chem. Phys.* **1992**, 96, 826.
32. Z. Kh. Ibragimova, E. M. Ivleva, N. V. jPavlova, T. A, Borodulina, V. A. Efremov, V. A. Kasaikin, A. B. Zezin, V. A. Kavanov, *Polymer Science*, **1992**, 34, 808.
33. J. Xia, P. L. Dubin, Y. Kim, *J. Phys. Chem.*, **1992**, 96, 6805.
34. W. Brown, J. Fundin, M. da Graca Miguel, *Macromolecules*, **1992**, 25, 7192.
35. W. Brown, K. Schillen, S. Hvidt, *J. Phys. Chem.* **1992**, 96, 6038.
36. B. Chu, *Polymer*, **1992**, 33, 4009.
37. Y. Deng, J. Ding, R. B. Stubbersfield, F. Heatley, D. Attwood, C. Price, C. Booth, *Polymer*, **1992**, 33, 1963.
38. A. Desjardins, T. G. M. van de Ven, A. Eisenberg, *Macromolecules*, **1992**, 25, 2412.
39. W. Richtering, R. Loffler, W. Burchard, *Macromolecules*, **1992**, 25, 3642.
40. J. Stejskal, D. Hlavata, A. Sikora, C. Konak, J. Plestil, P. Kratochvil, *Polymer*, **1992**, 33, 3675.
41. R. Xu, M. A. Winnik, G. Riess, B. Chu, M. D. Croucher, *Macromolecules*, **1992**, 25, 644.
42. L. Fang, W. Brown, S. Hvidt, *Macromolecules* **1992**, 25, 3137.
43. C. Konak, R. Bansil, S. Pajevic, *Polymer* **1992**, 33, 2238.
44. B. Nystrom, J. Roots, A. Carlsson, B. Lindman, *Polymer*, **1992**, 33, 2875.
45. H. Oikawa, *Polymer* **1992**, 33, 1116.
46. S. K. Patel, C. Cohen, *Macromolecules* **1992**, 25, 5252:
47. Y. Suzuki, K. Nozaki, T. Yamamoto, K. Itoh, I. Nishio, *J. Chem. Phys.*, **1992**, 97, 3808.

DISTRIBUTION LIST

No. of Copies	To
1	Office of the Under Secretary of Defense for Research and Engineering, The Pentagon, Washington, DC 20301
	Director, U.S. Army Research Laboratory, 2800 Powder Mill Road, Adelphi, MD 20783-1197
1	ATTN: AMSRL-OP-SD-TP, Technical Publishing Branch
1	AMSRL-OP-SD-TA, Records Management
1	AMSRL-OP-SD-TL, Technical Library
	Commander, Defense Technical Information Center, Cameron Station, Building 5, 5010 Duke Street, Alexandria, VA 23304-6145
2	ATTN: DTIC-FDAC
1	MIA/CINDAS, Purdue University, 2595 Yeager Road, West Lafayette, IN 47905
	Commander, Army Research Office, P.O. Box 12211, Research Triangle Park, NC 27709-2211
1	ATTN: Information Processing Office
	Commander, U.S. Army Materiel Command, 5001 Eisenhower Avenue, Alexandria, VA 22333
1	ATTN: AMCSCI
	Commander, U.S. Army Materiel Systems Analysis Activity, Aberdeen Proving Ground, MD 21005
1	ATTN: AMXSY-MP, H. Cohen
	Commander, U.S. Army Missile Command, Redstone Arsenal, AL 35809
1	ATTN: AMSMI-RD-CS-R/Doc
	Commander, U.S. Army Armament, Munitions and Chemical Command, Dover, NJ 07801
2	ATTN: Technical Library
	Commander, U.S. Army Natick Research, Development and Engineering Center, Natick, MA 01760-5010
1	ATTN: DFAS-IN-EM-TL, Technical Library
	Commander, U.S. Army Satellite Communications Agency, Fort Monmouth, NJ 07703
1	ATTN: Technical Document Center
	Commander, U.S. Army Tank-Automotive Command, Warren, MI 48397-5000
1	ATTN: AMSTA-ZSK
1	AMSTA-TSL, Technical Library
	President, Airborne, Electronics and Special Warfare Board, Fort Bragg, NC 28307
1	ATTN: Library
	Director, U.S. Army Research Laboratory, Weapons Technology, Aberdeen Proving Ground, MD 21005-5066
1	ATTN: AMSRL-WT

No. of Copies	To
	Commander, Dugway Proving Ground, UT 84022
1	ATTN: Technical Library, Technical Information Division
	Commander, U.S. Army Research Laboratory, 2800 Powder Mill Road, Adelphi, MD 20783
1	ATTN: AMSRL-SS
	Director, Benet Weapons Laboratory, LCWSL, USA AMCCOM, Watervliet, NY 12189
1	ATTN: AMSMC-LCB-TL
1	AMSMC-LCB-R
1	AMSMC-LCB-RM
1	AMSMC-LCB-RP
	Commander, U.S. Army Foreign Science and Technology Center, 220 7th Street, N.E., Charlottesville, VA 22901-5396
3	ATTN: AIFRTC, Applied Technologies Branch, Gerald Schlesinger
	Commander, U.S. Army Aeromedical Research Unit, P.O. Box 577, Fort Rucker, AL 36360
1	ATTN: Technical Library
	U.S. Army Aviation Training Library, Fort Rucker, AL 36360
1	ATTN: Building 5906-5907
	Commander, U.S. Army Agency for Aviation Safety, Fort Rucker, AL 36362
1	ATTN: Technical Library
	Commander, Clarke Engineer School Library, 3202 Nebraska Ave., N, Fort Leonard Wood, MO 65473-5000
1	ATTN: Library
	Commander, U.S. Army Engineer Waterways Experiment Station, P.O. Box 631, Vicksburg, MS 39180
1	ATTN: Research Center Library
	Commandant, U.S. Army Quartermaster School, Fort Lee, VA 23801
1	ATTN: Quartermaster School Library
	Naval Research Laboratory, Washington, DC 20375
2	ATTN: Dr. G. R. Yoder - Code 6384
	Chief of Naval Research, Arlington, VA 22217
1	ATTN: Code 471
	Commander, U.S. Air Force Wright Research & Development Center, Wright-Patterson Air Force Base, OH 45433-6523
1	ATTN: WRDC/MLLP, M. Forney, Jr.
1	WRDC/MLBC, Mr. Stanley Schulman
	U.S. Department of Commerce, National Institute of Standards and Technology, Gaithersburg, MD 20899
1	ATTN: Stephen M. Hsu, Chief, Ceramics Division, Institute for Materials Science and Engineering

No. of Copies	To
1	Committee on Marine Structures, Marine Board, National Research Council, 2101 Constitution Avenue, N.W., Washington, DC 20418
1	Materials Sciences Corporation, Suite 250, 500 Office Center Drive, Fort Washington, PA 19034
1	Charles Stark Draper Laboratory, 555 Technology Square, Cambridge, MA 02139
	Wyman-Gordon Company, Worcester, MA 01601
1	ATTN: Technical Library
	General Dynamics, Convair Aerospace Division, P.O. Box 748, Fort Worth, TX 76101
1	ATTN: Mfg. Engineering Technical Library
	Plastics Technical Evaluation Center, PLASTEC, ARDEC, Bldg. 355N, Picatinny Arsenal, NJ 07806-5000
1	ATTN: Harry Pebly
1	Department of the Army, Aerostructures Directorate, MS-266, U.S. Army Aviation R&T Activity - AVSCOM, Langley Research Center, Hampton, VA 23665-5225
1	NASA - Langley Research Center, Hampton, VA 23665-5225
	U.S. Army Vehicle Propulsion Directorate, NASA Lewis Research Center, 2100 Brookpark Road, Cleveland, OH 44135-3191
1	ATTN: AMSRL-VP
	Director, Defense Intelligence Agency, Washington, DC 20340-6053
1	ATTN: ODT-5A (Mr. Frank Jaeger)
	U.S. Army Communications and Electronics Command, Fort Monmouth, NJ 07703
1	ATTN: Technical Library
	U.S. Army Research Laboratory, Electronic Power Sources Directorate, Fort Monmouth, NJ 07703
1	ATTN: Technical Library
	Director, U.S. Army Research Laboratory, Watertown, MA 02172-0001
2	ATTN: AMSRL-OP-WT-IS, Technical Library
5	Authors